The transcription factor Foxc1a in zebrafish directly regulates expression of *nkx2.5*, encoding a transcriptional regulator of cardiac progenitor cells

Yunyun Yue, Mingyang Jiang, Luqingqing He, Zhaojunjie Zhang, Qinxin Zhang, Chun Gu, Meijing Liu, Nan Li, and Qingshun Zhao[1]

From the Model Animal Research Center, Ministry of Education Key Laboratory of Model Animal for Disease Study, Nanjing University, 12 Xuefu Road, Pukou High-tech Development Zone, Nanjing 210061, China

Edited by Xiao-Fan Wang

Cardiogenesis is a tightly controlled biological process required for formation of a functional heart. The transcription factor Foxc1 not only plays a crucial role in outflow tract development in mice, but is also involved in cardiac structure formation and normal function in humans. However, the molecular mechanisms by which Foxc1 controls cardiac development remain poorly understood. Previously, we reported that zebrafish embryos deficient in *foxc1a*, an ortholog of mammalian *Foxc1*, display pericardial edemas and die 9–10 days postfertilization. To further investigate Foxc1a's role in zebrafish cardiogenesis and identify its downstream target genes during early heart development, we comprehensively analyzed the cardiovascular phenotype of *foxc1a*-null zebrafish embryos. Our results confirmed that *foxc1a*-null mutants exhibit disrupted cardiac morphology, structure, and function. Performing transcriptome analysis on the *foxc1a* mutants, we found that the expression of the cardiac progenitor marker gene *nkx2.5* was significantly decreased, but the expression of germ layer–patterning genes was unaffected. Dual-fluorescence *in situ* hybridization assays revealed that *foxc1a* and *nkx2.5* are co-expressed in the anterior lateral plate mesoderm at the somite stage. Chromatin immunoprecipitation and promoter truncation assays disclosed that Foxc1a regulates *nkx2.5* expression via direct binding to two noncanonical binding sites in the proximal *nkx2.5* promoter. Moreover, functional rescue experiments revealed that developmental stage–specific *nkx2.5* overexpression partially rescues the cardiac defects of the *foxc1a*-null embryos. Taken together, our results indicate that during zebrafish cardiogenesis, Foxc1a is active directly upstream of *nkx2.5*.

Cardiogenesis is a complex process consisting of a series cellular specification, differentiation, and morphogenesis. Similar to mammalian heart development, zebrafish cardiac progenitors emerge earliest from late blastula stage (1). Along with cardiac progenitor cell migration, differentiation, and proliferation, two-chambered zebrafish heart starts to work from 24 hpf[2]. Because they have rapid early heart development and can survive for almost 1 week without a functioning cardiovascular system, zebrafish have become an increasingly popular model for cardiovascular research.

Foxc1 is a member of the FOX transcription factors with a conserved forkhead domain (2). It not only plays important roles in vertebrate heart development, but also is involved in cardiac structure formation and normal function in humans (3). Mice carrying *Foxc1* null alleles die at birth with hydrocephalus, skeletal abnormalities, and heart defects. Mouse *Foxc1* and *Foxc2* function redundantly in regulating the expression of *Tbx1* in out-flow tract morphogenesis (4–6). Zebrafish *foxc1a*-knockout embryos display severe heart defects (7). In humans, some patients carrying the *FOXC1* single allele mutation suffer from different kinds of cardiac anomalies, including mild dysplasia of the left ventricle, OFT, valvula tricuspidalis, and heart failure (8–10). Recently, in the induction of human ES cells into cardiomyocytes, FOXC1 is essential for the differentiation by regulating the expression of *MYH7* (11). Analysis of RNA profiles from human failing and non-failing heart suggests specific roles of FOX transcription factors (FOXC1, C2, P1, P4, and O1A) in modulating the human heart failure pathogenesis by regulating the expressions of key factors, such as MEF2, NKX, NF-AT, and GATA (12).

Although *Foxc1* plays essential roles in cardiogenesis and cardiac pathology, little is known about the molecular mechanisms underlying its roles (5, 13, 14). Nkx2-5 is one of the most pivotal regulators during vertebrate cardiac progenitor cell (CPC) specification and cardiomyocyte differentiation. *Nkx2-5* knockout mice die at embryonic day 10.5 with only a single ventricle and defects of OFT (15). Postnatal mice with conditional knockout of *Nkx2-5* exhibit a disturbed heart conduction system (16, 17). Mutation of *nkx2.5* in zebrafish disrupts the cardiac morphogenesis, exhibiting a small, constricted ventricle and a dilated atrium (18). Zebrafish embryos with double null genes of *nkx2.5* and *nkx2.7* almost do not form the ventricle (19). Lots of *NKX2-5* mutations have been discovered in human congenital heart disease patients (20–22).

[2] The abbreviations used are: hpf, hours postfertilization; CPC, cardiac progenitor cell; OFT, out-flow tract; EI, edema index; SF, shortening fraction; AVC, atrio-ventricular canal; VD, ventricular diastole; VS, ventricular systole; ALPM, anterior lateral plate mesoderm; LPM, lateral plate mesoderm; ISH, *in situ* hybridization; eYFP, enhanced YFP.

The dynamic expression of *NKX2-5* is known to be tightly controlled in vertebrate heart. In addition to signaling pathways, such as retinoic acid and WNT, that act upstream of *Nkx2.5* to regulate CPC specification (23–25), transcription factors like FOXP1 and the post-transcriptional regulation mechanism are also involved in its expression regulation (26, 27). In this study, by comprehensively characterizing the disrupted heart structure and function in *foxc1a*-null zebrafish embryos, we demonstrate that Foxc1a controls zebrafish cardiogenesis by directly regulating *nkx2.5* expression.

Results

Zebrafish foxc1a-null embryos exhibit severe cardiovascular defects

Previously, we reported that *foxc1a*-null zebrafish embryos exhibit abnormal somitogenesis and heart development (7). Morphologically, the mutant embryos could be distinguished from their wild-type siblings earliest from 50 hpf due to their obvious pericardium edema (Fig. 1, *A* and *B*). Additionally, *foxc1a* mutants displayed shorter body length and smaller eyes at 72 hpf (Fig. S1). When reaching 108 hpf, the mutants exhibited more serious edema than their wild-type siblings (Fig. 1, *C* and *D*). The edema index (EI; defining the extent of pericardium edema) (28) of *foxc1a* mutant embryos was significantly ($p < 0.0001$) higher than that of their wild-type siblings at 108 hpf (Fig. 1*G*). Histologically, the mutant hearts displayed thinner myocardium layers, shorter OFT (Fig. 1, *E* and *F*), and defective primitive valve leaflets in which the endothelial cells only accumulated in the atrio-ventricular canal (AVC) rather than forming leaflets and extending into the ventricle (Fig. 1, *E*, *F*, *E′*, and *F′*).

To evaluate whether the heart functions were affected in *foxc1a* mutants, we first examined the heart rates at different developmental stages. We found that the heart rates of mutant embryos were comparable with wild-type siblings at 50 hpf ($p = 0.7714$) and 108 hpf ($p = 0.4358$), respectively (Fig. 1*H*). However, the heart rates of mutant embryos at 132 hpf were decreased dramatically ($p = 0.0089$) compared with their wild-type siblings (Fig. 1*H*). The results indicated that the reduction of heart rate was the consequence of heart defects but not the reason for cardiac malformation in *foxc1a* mutants.

We then analyzed the ventricle minor axis shortening fraction (SF) to validate the ventricle contraction ability of zebrafish embryos. The results showed that the ventricular SFs of *foxc1a* mutant embryos were significantly lower than that of their wild-type siblings at both 50 hpf ($p = 0.001$) and 108 hpf ($p = 0.0071$), respectively (Fig. 1*I*). These data elucidated that the heart contraction function was severely disrupted in *foxc1a*-null zebrafish embryos from 50 hpf. Taken together, our data demonstrate that Foxc1a deficiency resulted in heart defects, including both disorganized structures and disrupted functions in zebrafish embryos.

Heart chamber morphogenesis and AVC specification were disrupted in foxc1a mutant zebrafish embryos

To explore when the heart malformation occurs in *foxc1a*-null zebrafish embryos, we observed the heart morphogenesis in the embryos of *Tg(myl7:eGFP)^{m225};foxc1a^{nju19}* at 50 hpf. To rule out the size difference in different heart contract phases, we examined the heart sizes of the 50-hpf embryos at both ventricular diastole (VD) and systole (VS) phases. The results showed that both atrium and ventricle of *foxc1a* mutant embryos could form, but the size of the ventricle was smaller and that of the atrium was larger than in their wild-type siblings, respectively (Fig. 2, *A*, *B*, *A′*, and *B′*). Measuring the cross-sectional areas of heart chambers at VD phase, we found that the ventricle area of the mutant embryos was significantly smaller ($p < 0.0001$), whereas the atrium area was significantly larger ($p = 0.0015$) than in their wild-type siblings (Fig. 2*D*). Similar results were found at VS phase (Fig. 2*C*). On the other hand, we examined the expressions of the molecular markers for the formation of cardiac chambers in the embryos at 30 and 50 hpf, respectively. The results showed that the chamber-specific myosin heavy chain marker genes, including *amhc* (marker for atrial chamber) and *vmhc* (marker for ventricular chamber), were all expressed in *foxc1a* mutant embryos at both stages (Fig. 2*E*). However, the *amhc* expression area was larger, whereas the *vmhc* expression area was smaller in the mutant embryos than in their wild-type siblings (Fig. 2*E*). The results are consistent with the morphologic observation in the embryos of *Tg(myl7: eGFP)^{m225}; foxc1a^{nju19}* transgenic zebrafish (Fig. 2, *A–D*, *A′*, and *B′*), suggesting that Foxc1a is essential for regulating the size of two cardiac chambers and that the myocardium malformation should emerge from the earlier period of chamber differentiation no later than 30 hpf.

Hemodynamic changes, such as the malformation of vasculogenesis and blood flow, are known to affect heart development (29, 30). We therefore first investigated whether vasculogenesis and angiogenesis were normal in *foxc1a* mutants by observing endothelial cells in the embryos of *Tg(kdrl:eGFP)^{s843}; foxc1a^{nju19}*. The results showed that the mutant embryos exhibited normal trunk vasculogenesis but with only an angiogenesis defect in the head at both 30 hpf (Fig. S2, *A*, *B*, *A′*, and *B′*) and 50 hpf (Fig. S2, *C*, *D*, *C′*, and *D′*). They suggested that zebrafish *foxc1a* is critical for angiogenesis in the head region but dispensable in the trunk. Unlike the abnormal expression patterns of the marker genes for myocardium occurring in the *foxc1a*-null embryos at both 30 and 50 hpf (Fig. 2*E*), the expression pattern of *kdrl* (marker for endocardium) was similar to those of their wild-type siblings at 30 hpf (Fig. S2, *A*, *B*, *A′*, and *B′*). However, its expression level was significantly decreased in the mutant embryos at 50 hpf (Fig. S2, *C*, *D*, *C′*, and *D′*).

It is reported that there is visible blood in *Foxc1/2* mutant mice (4). Similarly, our study also found that blood flow could be observed in *foxc1a* mutant zebrafish embryos at 50 hpf (Movies S1 and S2). However, hemoglobin marker gene *hbae1* expression was significantly decreased in *foxc1a*-null embryos at both 30 and 50 hpf (Fig. S3, *C–F*). *o*-Dianisidine staining also showed that the erythrogenesis was affected in *foxc1a* mutant embryos at 50 hpf (Fig. S3, *A*, *B*, *A′*, and *B′*). We next examined the possible changes of blood flow shear force by checking the expression of *klf2a*, a marker gene expressed in the AVC region, in the mutant embryos at 50 hpf (29). We found that both mutant embryos and their wild-type siblings exhibited similar expressions of *klf2a* in AVC (Fig. 2*G*). These results indicated that the angiogenesis defects in the head and the abnormal
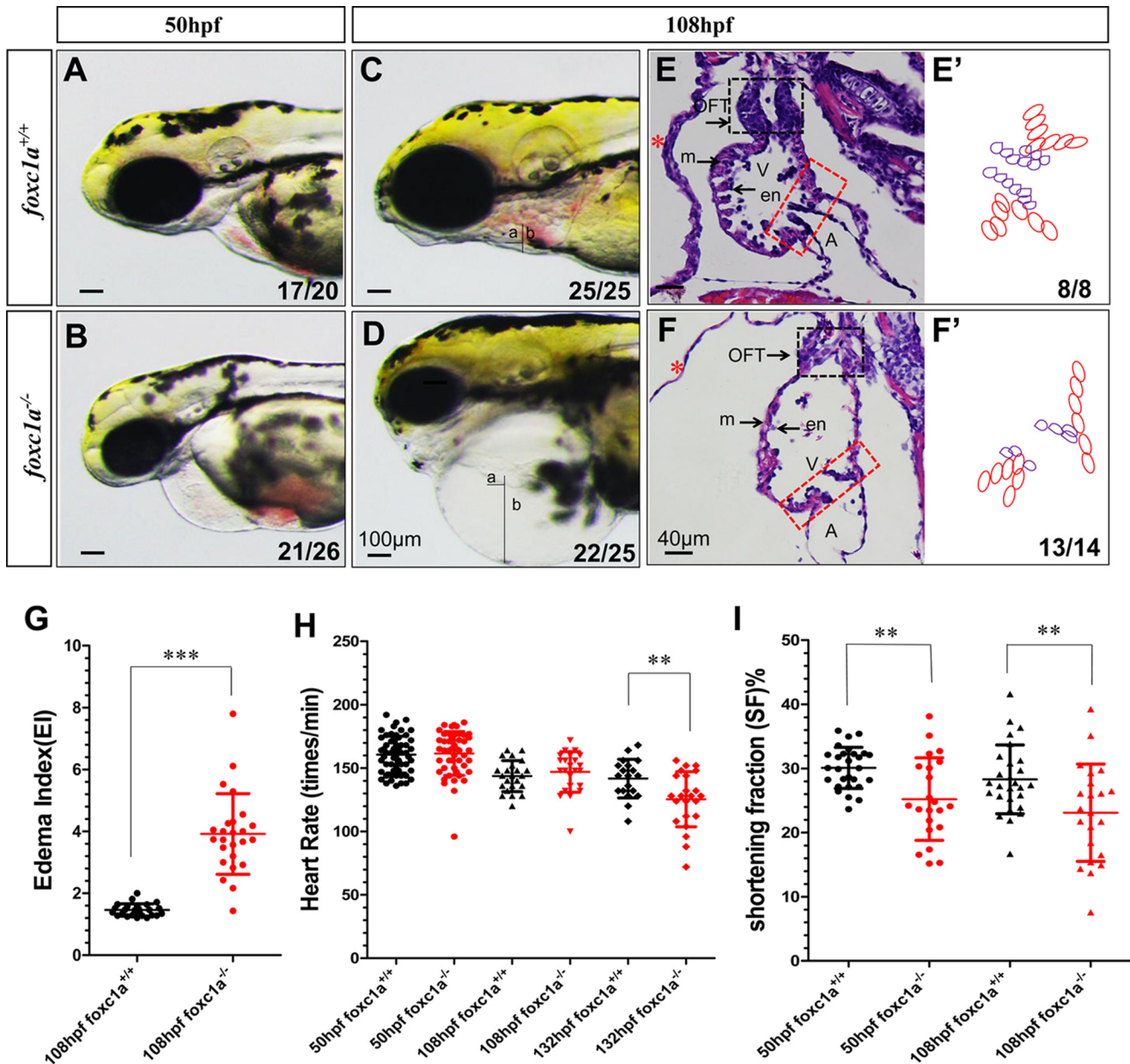
Figure 1. Foxc1a knockout zebrafish embryos exhibit severe cardiovascular defects. *A–D*, lateral views of wild-type siblings (*A* and *C*) and *foxc1a* knockout mutants (*B* and *D*) at 50 hpf (*A* and *B*) and 108 hpf (*C* and *D*); *a*, the semidiameter of ventricle; *b*, the semidiameter of the pericardial cavity. *E* and *F*, section of heart of wild type (*E*) and mutants (*F*) at 108 hpf. *E'* and *F'*, schematic of the AVC region in wild type (*E'*) and mutants (*F'*) at 108 hpf. The *red cells* in the *outside* are myocardium, and the *purple cells* in the *inner region* are endocardium. *Red asterisk*, pericardial membrane; *A*, atrium; *V*, ventricle; *my*, myocardium; *en*, endocardium. *Rectangle outlined* with *red dots*, valve leaflets; *rectangle outlined* with *black dots*, OFT region. The *number* in the *bottom right corner* of each *panel* is the number of embryos with typical phenotype in total observed ones. *G*, scatter plot showing the value of EI in wild type (*n* = 25) and mutants (*n* = 25) at 108 hpf. *H*, scatter plot showing heart rates in wild type (*black dots*) and mutants (*red dots*) at 50 hpf (*n* = 48 in wild type and *n* = 57 in mutants), 108 hpf (*n* = 23 in wild type and *n* = 23 in mutants), and 132 hpf (*n* = 19 in wild type and *n* = 23 in mutants), respectively. *I*, scatter plot showing the value of ventricle minor axis SF in wild type and mutants at 50 hpf (*n* = 23 in wild type and *n* = 28 in mutants) and 108 hpf (*n* = 22 in wild type and *n* = 27 in mutants). **, *p* < 0.01; ***, *p* < 0.001. *Error bars*, S.D.

erythrogenesis were not the cause of heart malformation in *foxc1a* mutant embryos.

AVC is a specific heart region that connects the atrium and ventricle and gives rise to primitive leaflets that prevent the blood flow from retrograding (31). It is specified at 37 hpf shortly after the linear heart tube of zebrafish embryo starts to loop from 36 hpf (32). Due to the defective valve leaflets in *foxc1a*-null embryos, we examined whether AVC was normally specified in the mutant embryos. To do this, we first examined the expression of *myl7*, a marker gene for heart looping, in the

mutant embryos. The results showed that the *fox1a* mutants exhibited an abnormal expression pattern of *myl7* at 50 hpf, although its expression was normal at 30 hpf (Fig. 2*E*). Consistently, the chamber-specific gene *nppa* was expressed ectopically in the AVC of *foxc1a*-null embryos at 50 hpf (Fig. 2*F*). The results suggest that AVC malformation occurred in the mutant embryos. To confirm this conclusion, we examined the expression patterns of AVC-specific markers in the *foxc1a* mutant embryos and wild-type siblings at 50 hpf. The results revealed that the expressions of myocardium AVC-specific genes *bmp4*
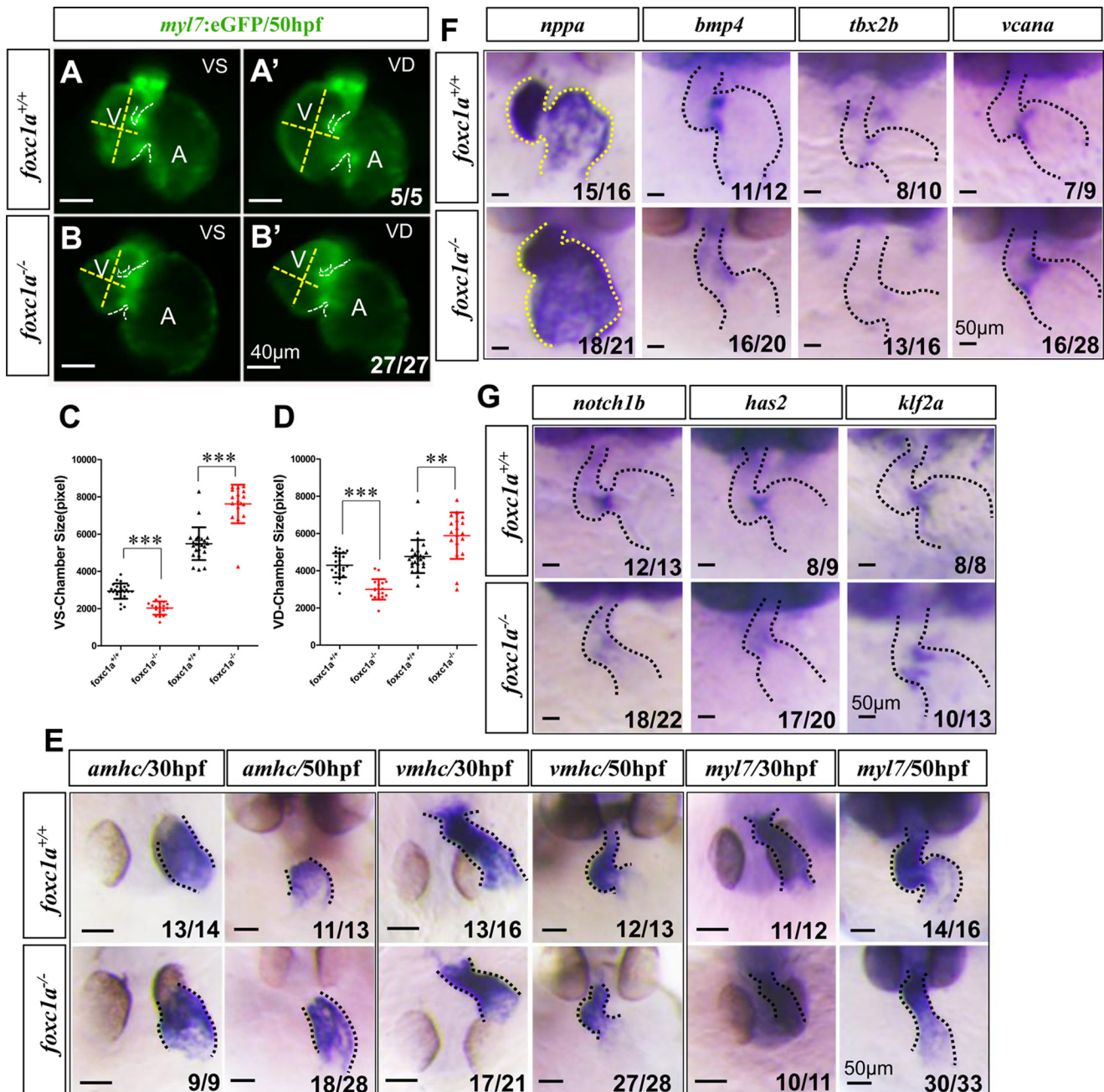
Figure 2. The morphogenesis of heart chamber and AVC specification are disrupted in *foxc1a*-knockout mutants. *A*, *B*, *A'*, and *B'*, ventral view of heart of wild-type siblings (*A* and *B*) and *foxc1a* mutant embryos (*A'* and *B'*) under fluorescence microscopy in *Tg(myl7:eGFP)^{m225}* transgenic background at 50 hpf. The *yellow dotted line* indicates the length and width of ventricle. The *white dotted curve* denotes the outline of AVC. *A*, atrium; *V*, ventricle. *C* and *D*, scatter plot showing the relative areas of atrium (*triangle*) or ventricle (*dot*) at the VS or VD phase of embryos at 50 hpf (*n* = 26 in wild type (*black*) and *n* = 18 in mutants (*red*)). *E*, whole-mount *in situ* hybridized embryos showing the expressions of *amhc*, *vmhc*, and *myl7* in the embryos at 30 and 50 hpf, respectively. The *curve outlined* by *black dots* shows the outline of the expression regions of marker genes. *F*, whole-mount *in situ* hybridized embryos showing the expressions of AVC marker genes, including *nppa*, *bmp4*, *tbx2b*, and *vcana*. *G*, whole-mount *in situ* hybridized embryos showing the expressions of *noth1b*, *has2*, and *klf2a* in AVC regions of wild-type siblings and *foxc1a*-null embryos. The number of embryos in the *bottom right corner* of each *panel* is the number of embryos with typical phenotype of the total observed embryos. **, *p* < 0.01; ***, *p* < 0.001. Error bars, S.D.

and *tbx2b* (Fig. 2*F*) and endocardium AVC-specific genes *notch1b* and *has2* (Fig. 2*G*) were all significantly reduced in *foxc1a* mutants. However, the expression of *vcana* was ectopically expanded into the ventricular chamber (Fig. 2*F*) in the mutant embryos at 50 hpf. Taken together, our results demonstrated that the heart chamber differentiation and AVC specification are abnormal in *foxc1*a mutants, and the abnormal

heart development should occur at an earlier developmental stage no later than 30 hpf.

The specification of cardiac progenitors was disrupted in *foxc1a* mutants

It has been reported that knockdown of *FOXC1* leads to the decreased expression of mesoderm-specific genes (33). To test
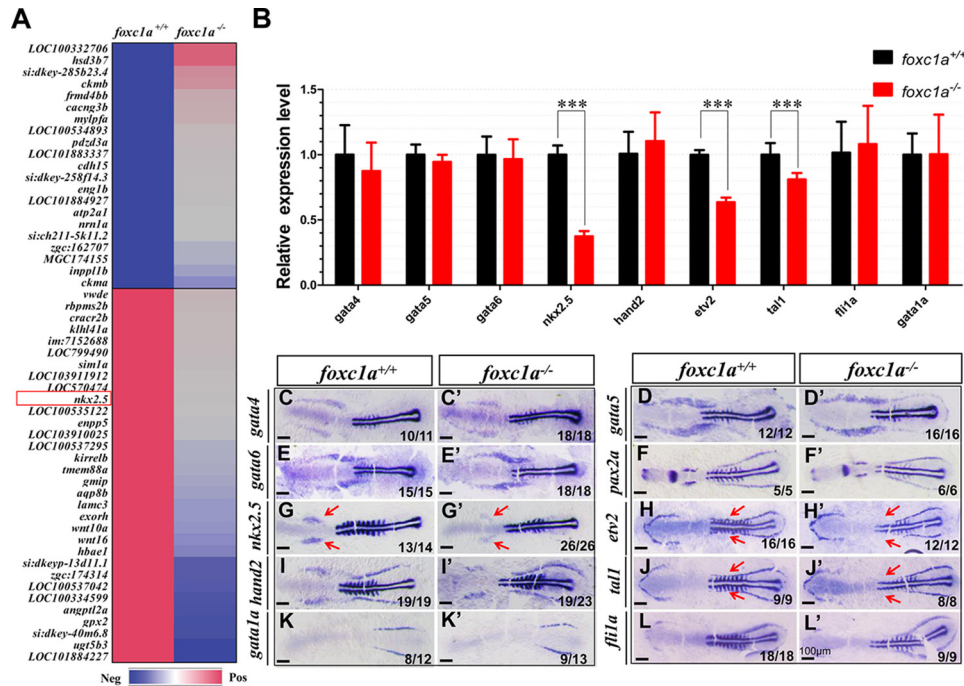
Figure 3. The expression of *nkx2.5* is significantly decreased in ALPM of *foxc1a*-null embryos at the 10-somite stage. *A*, heat map shows the 21 up-regulated genes and 32 down-regulated genes (-fold change > 3, *p* < 0.05) in *foxc1a*-null embryos identified by an RNA-seq assay at the 10-somite stage. *B*, quantitative real-time PCR results showing the expressions of *gata4*, *gata5*, *gata6* (at the six-somite stage), *etv2*, *tal1*, *hand2*, *fli1a*, *nkx2.5*, and *gata1a* (at the 10-somite stage) in *foxc1a*-null embryos and their siblings. *C–L*, whole-mount *in situ* hybridized embryos showing the expression patterns of *gata4*, *gata5*, *gata6* (at the six-somite stage), *pax2a* (at the eight-somite stage), *nkx2.5*, *hand2*, *etv2*, *tal1*, *fli1a*, and *gata1a* (at the 10-somite stage) in LPM of *foxc1a*-null embryos and their siblings. All embryos were co-hybridized with *myod1* to label the somite except in *K* and *K'*. The number in the *bottom right corner* of each *panel* is the number of embryos with typical phenotype of the total observed embryos. ***, *p* < 0.001. *Error bars*, S.D.

whether Foxc1a play essential roles in mesoderm formation of zebrafish embryos, we examined the expressions of some germ layer differentiation genes in the mutant embryos. Results from whole-mount *in situ* hybridization of the representative marker genes for mesoderm (*ta*, *gsc*, *dkk1b*, *noto*, and *gata5*), endoderm (*pou5f3*, *mixl1*, *sox32*, and *sox17*), and ectoderm (*zic1*) (Fig. S4) showed that the formation of the three germ layers were normal in *foxc1a* mutant embryos at 6 hpf. Consistently, analysis on the transcriptome of the *foxc1a*-null embryos at 6 hpf further indicated that the expression of germ layer–patterning genes was unaffected in the mutant embryos compared with wild-type siblings at the gastrulation stage (data not shown).

Now that the heart defects in *foxc1a*-null embryos were found to occur no later than 30 hpf (Fig. 2*E*) and the germ layer formation, especially mesoderm formation, looked normal in the mutant embryos (Fig. S4), it was reasonable for us to hypothesize that Foxc1a contributes to heart development via affecting the specification of cardiac progenitors. Cardiac progenitors specified from lateral plate mesoderm will differentiate to cardiomyocytes in vertebrate. To test this hypothesis, we compared the transcriptome of *foxc1a* mutants with their wild-type siblings at 14 hpf when the cardiac progenitors are specified in the caudal end of the anterior lateral plate mesoderm (ALPM) of zebrafish embryos. The result showed that the expression of cardiac progenitor marker gene *nkx2.5* was decreased significantly (Fig. 3*A*), and those of other well-known ALPM related genes such as *etv2* and *tal* were mildly downregulated in *foxc1a* mutants (data not shown). To confirm the

RNA-seq result, we examined the expression patterns of *nkx2.5*, *etv2*, and *tal1* in the *foxc1a* mutants and wild-type siblings. Consistent with the RNA-seq result, whole-mount *in situ* hybridization analysis revealed that the expression of *nkx2.5* was significantly reduced in the caudal portion of ALPM (Fig. 3, *G* and *G'*), and those of *etv2* and *tal1* (for specifying the progenitors of endocardium, head endothelium, and primitive myelopoiesis) were decreased in medial LPM, although the two genes had almost no change in the rostral portion of ALPM in the *foxc1a*-null embryos (Fig. 3, *H*, *J*, *H'*, and *J'*). Quantitative realtime PCR analysis revealed that the expression levels of *nkx2.5*, *etv2*, and *tal1* were decreased to 25.0, 63.5, and 81.1% in the *foxc1a*-null embryos compared with their wild-type siblings, respectively (Fig. 3*B*).

To exclude the possibility that the abnormal expression patterns of *nkx2.5*, *etv2*, and *tal1* were due to the defective specification of ALPM, we examined the expressions of ALPM marker genes, including *gata4*, *gata5*, and *gata6*, in the mutant embryos and their wild-type siblings. The results from both quantitative real-time PCR and whole-mount *in situ* hybridization revealed that the expression levels and patterns of all of the three genes in the *foxc1a*-null embryos were the same as their wild-type siblings at the six-somite stage (Fig. 3, *B*, *C–E*, and *C'–E'*). The results suggested that the ALPM was normally formed in *foxc1a*-null embryos. Consistent with the normal formation of ALPM, the results from whole-mount *in situ* hybridization demonstrated that the expressions of *pax2a* (Fig. 3, *F* and *F'*), a marker gene for PLPM, and *hand2* (Fig. 3, *I* and *I'*), a second key regulator for the specification of cardiac progeni-
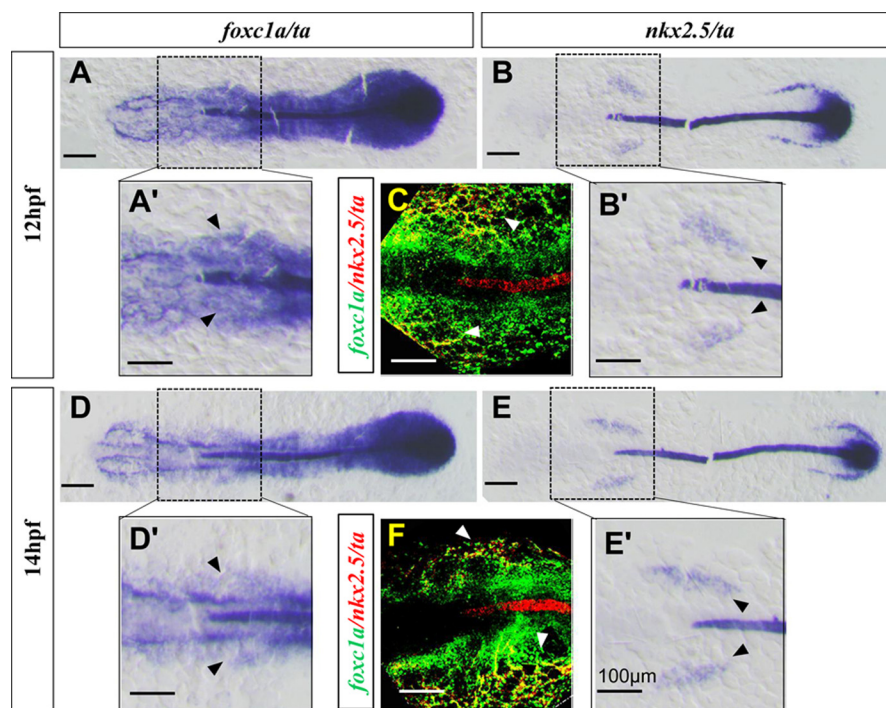
Figure 4. Zebrafish *foxc1a* is co-expressed with *nkx2.5* in the caudal portion of ALPM at somite stage. *A, B, D,* and *E,* expressions of *foxc1a* at 12 hpf (*A*) and 14 hpf (*D*) and of *nkx2.5* at 12 hpf (*B*) and 14 hpf (*E*). *A′–D′,* magnification of the expression in LPM. *C* and *F,* double florescence ISH of *foxc1a* and *nkx2.5* in wild-type zebrafish embryos at 12 hpf (*C*) and 14 hpf (*F*). Embryos were co-stained with *ta* probe to indicate the midline (*A–F*). The *black arrowhead* indicates the expressions of *foxc1a* (*A′* and *D′*) and *nkx2.5* (*B′* and *E′*). The *white arrowhead* indicates the *merged yellow signal* with *green foxc1a* expression and *red nkx2.5* expression (*C* and *F*).

tors, were both normal in *foxc1a* mutants. Additionally, results from both quantitative real-time PCR and whole-mount *in situ* hybridization revealed that the expression of *gata1a*, a marker gene for the formation of red blood progenitors (Fig. 3, *B, K,* and *K′*), and *fli1a*, the endothelial cell marker gene (Fig. 3, *B, L,* and *L′*), had no obvious change in ALPM and PLPM of *foxc1a*-null embryos. Taken together, our results demonstrate that *foxc1a* depletion does not affect the formation of mesoderm but influences the specification of cardiomyoblast in the caudal end of ALPM of zebrafish embryos by reducing the expression of *nkx2.5*.

Zebrafish foxc1a is co-expressed with nkx2.5 in the caudal end of ALPM

Zebrafish *foxc1a* is a zygotic gene that is expressed from 30% epiboly (data not shown). When the embryos grow to the 50% epiboly stage, the expression of *foxc1a* is mainly in the marginal zone of the meso-endoderm (Fig. S5*A*), and then the mesoderm in the embryos at 75% epiboly (Fig. S5*B*). At the somite stage, *foxc1a* is expressed in the paraxial mesoderm (Fig. S5, *C* and *D*). When the embryos reach 24 hpf, the *foxc1a* is dominantly expressed in the endothelial cells of the head and trunk and the eyes. At 50 hpf, the embryos exhibit weak expression of *foxc1a* in the heart in addition to its expression in the endothelial cells.

To investigate whether Foxc1a regulates the expression of *nkx2.5* in the caudal part of ALPM directly, we first examined whether the two genes were co-expressed in zebrafish embryos at somite stage. By visualizing the expressions of *nkx2.5* and *foxc1a* in the wild-type embryos at 12 and 14 hpf using the Cy5

(observed by *red color*) channel and fluorescein (observed by *green color*) channel of the confocal microscope, respectively (*ta* was co-stained by Cy5), we found that some green fluorescent cells also harbored red fluorescence (Fig. 4, *H–M* and *H′–K′*). The results suggested that *foxc1a* and *nkx2.5* were co-expressed in at least part of the cells in the caudal portion of ALPM.

Foxc1a controls the expression of nkx2.5 by binding to its promoter in zebrafish embryos at somite stage

To determine whether *nkx2.5* is a direct target gene of Foxc1a that controls heart development, we next determined whether Foxc1a regulates *nkx2.5* expression by directly binding to its promoter. Performing a Dual-Luciferase assay to examine the activities of truncated promoters of zebrafish *nkx2.5* with different lengths in response to Foxc1a, we found that the *nkx2.5* promoter with diverse lengths (1908, 1462, 1120, 629–1120, and 629 bp) could all be activated by overexpression of wild-type *foxc1a* mRNA (Fig. 5*A*). In contrast, the 1120-bp promoter activity could not be regulated by *foxc1a* mutant mRNA (Fig. S6*A*). The results suggest that there are binding sites of Foxc1a in the 1120-bp fragment.

To identify the binding sites of Foxc1a, we performed a ChIP assay on the chromatin isolated from zebrafish embryos at the 10-somite stage using antibody against zebrafish Foxc1a. The results showed that Foxc1a was significantly enriched in the fragment of S1 (-1 to -172 bp) and S5 (-624 to -782 bp) region of zebrafish *nkx2.5* promoter (Fig. 5*B*). To confirm the results, we performed the Dual-Luciferase assay on the mutated 1120-bp promoter in which either S1 or S5 was deleted or both
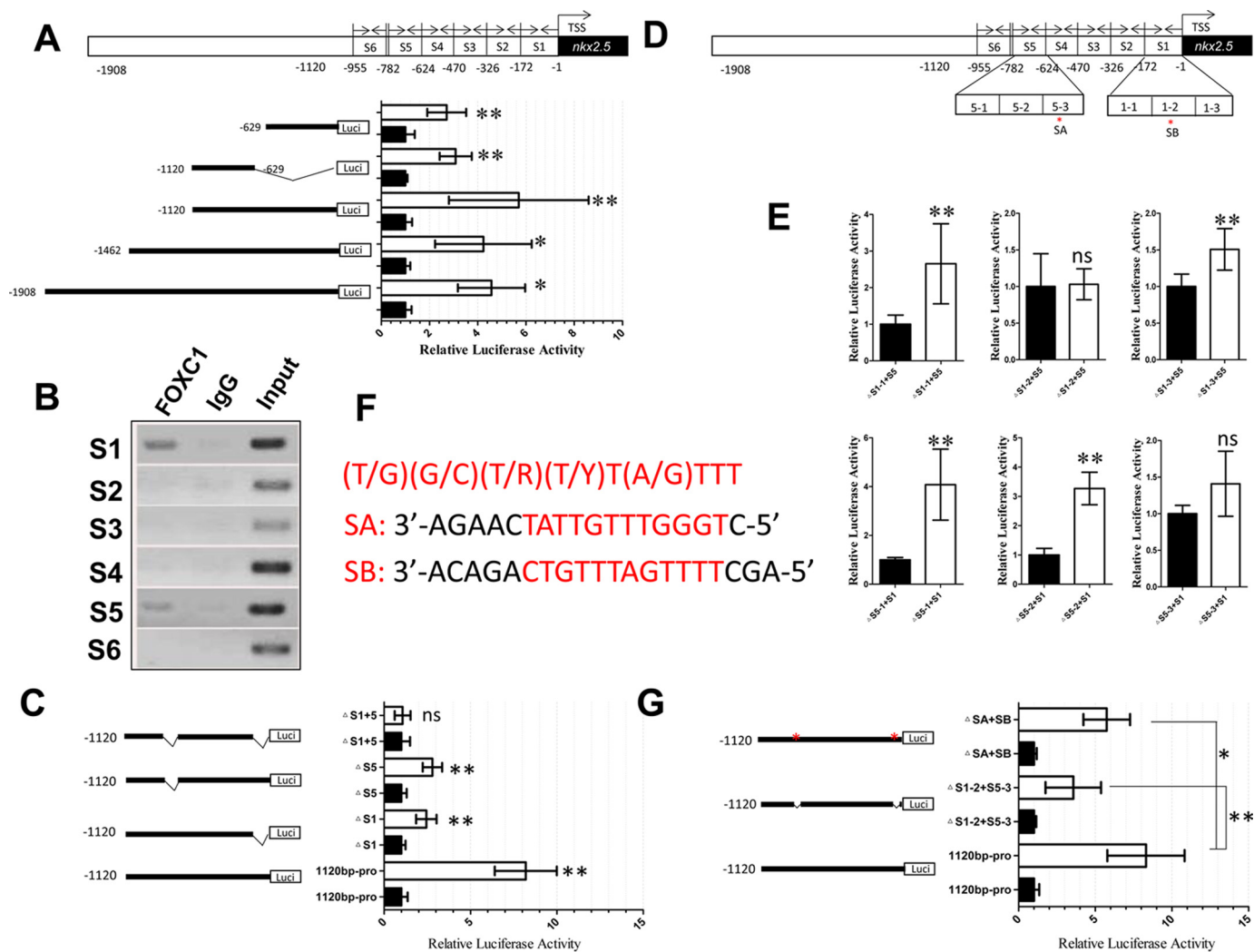
Figure 5. The expression of *nkx2.5* is directly regulated by Foxc1a in the specification of cardiac progenitors. *A*, *schematic diagram* showing the zebrafish *nkx2.5* promoter (*top*) and Dual-Luciferase assay showing its response to Foxc1a (*bottom*). *S1–S6*, the PCR amplification region in the ChIP-PCR assay (*B*). *TSS*, transcription start site. The *black lines* indicate different lengths of *nkx2.5* promoter that were cloned into the pGL3-basic vector for the Dual-Luciferase assay. *B*, ChIP-PCR assay indicating that S1 and S5 may be the two possible Foxc1a-binding regions in the *nkx2.5* promoter. *C*, Dual-Luciferase assay showing the activities of the 1120-bp promoter, 1120-bp promoter without S1 region, 1120-bp promoter without S5 region, and 1120-bp promoter without either S1 or S5 region in response to Foxc1a. *D*, schematic diagram shows dissection of *nkx2.5* promoter S1 region into S1-2, S1-2, and S1-3 and the S5 region into S5-1, S5-2, and S5-3. The *red asterisk* in *D* and *G* shows the two putative Foxc1a-binding sites SA and SB present in *nkx2.5* promoter regions. *E*, the Dual-Luciferase assay was performed with mutated promoters of S1-1 and S5 deletion, S1-2 and S5 deletion, S1-3 and S5 deletion, S1 and S5-1 deletion, S1 and S5-2 deletion, and S1 and S5-3 deletion in wild-type zebrafish embryos. *F*, the core sequences of the conserved Foxc1 transcription factor binding sequence in vertebrates and in zebrafish *nkx2.5* promoter regions of SA and SB. *G*, Dual-Luciferase assay was performed with 1120-bp promoter, S1-2 and S5-3 deletion, and SA and SB deletion in wild-type zebrafish embryos. *Black histogram*, control activity that was normalized as 1.0; *white histogram*, activity derived from the embryos co-microinjected with 20 pg of *foxc1a* mRNA plus the promoter. *, $p < 0.05$; **, $p < 0.01$; *ns*, not significant. *Error bars*, S.D.

S1 and S5 were deleted. Consistent with the ChIP results (Fig. 5B), the mutated promoters with deletion of either S1 or S5 were still activated by Foxc1a, although their activities were significantly ($p < 0.05$) lower than that of the wild-type 1120-bp promoter (Fig. 5C), respectively. However, the mutated promoter with double deletion of S1 and S5 had no response ($p > 0.05$) to Foxc1a (Fig. 5C).

To further identify the core sequences of Foxc1a-binding sites in the *nkx2.5* promoter region, we dissected the S1 and S5 region into three regions and then performed a Dual-Luciferase assay to examine the truncated promoter activities in response to Foxc1a, respectively (Fig. 5D). The results showed that S1-2 and S5-3 should contain binding sites of Foxc1a (Fig. 5E). Previously, it was reported that the core

sequence of the Foxc1a-binding sites is (T/G)(G/C)(T/R)(T/Y)T(A/G)TTT (34). Performing bioinformatics analysis, we found that there were two putative non-canonical binding sites, namely SA (TATTGTTTGGGT) in S5-3 and SB (CTGTTTAGTTT) in S1-2, respectively (Fig. 5F). To verify that they were the real core sequence of Foxc1a-binding sites in zebrafish *nkx2.5* promoter, we made new promoter constructs by deleting S1-2 and S5-3 or SA and SB (Fig. 5G) and then performed the Dual-Luciferase assay to examine their responses to Foxc1a, respectively. The results revealed that the luciferase activities were significantly decreased ($p < 0.05$) in the S1-2 and S5-3 double deletion or the SA and SB double deletion group compared with the 1120-bp wild-type promoter group, respectively (Fig. 5G).

Overexpression of nkx2.5 could partially rescue the cardiac defects in foxc1a mutant embryos

To verify that the heart defects in *foxc1a* mutant zebrafish embryos result (at least partially) from the reduction of the *nkx2.5* expression in ALPM of *foxc1a*-null embryos at the somite stage, we microinjected the transgenic construct comprising the *hsp70l* (heat shock protein 70-like) promoter to drive the expression of Nkx2.5-P2A-eYFP (Fig. 6A) into the embryos at the one-cell stage derived from incross of *Tg(kdrl: eGFP)^{s843}*; *foxc1a^{nju19/+}* zebrafish and then performed heat shock (37 °C) for 1 h from 10 hpf (18). Up to 14 hpf, the embryos with yellow fluorescence were selected for further experiment, and the embryos without heat shock activation were selected as the control group (Fig. 6, *B* and *C*). When they grew to 50 hpf, the embryos were measured to calculate their areas of atrium and ventricle at the VS and VD stage (Fig. 6A). The results showed that the size of the ventricle in *foxc1a* mutant embryos was increased significantly ($p < 0.0001$) after overexpression of *nkx2.5* and became similar to that of wild-type siblings overexpressed with *nkx2.5* ($p = 0.1689$) at VS stage (Fig. 6D). However, the size of the atrium in *foxc1a* mutant embryos was not changed ($p = 0.1121$) at the VS stage after overexpression of *nkx2.5* (Fig. 6E). Similarly, the size of ventricle in *foxc1a* mutant embryos was increased significantly ($p < 0.0001$) due to overexpression of *nkx2.5*, which became comparable with that of wild-type siblings ($p = 0.8564$) at the VD stage (Fig. 6D′). The size of the atrium in *foxc1a* mutant embryos was not changed ($p = 0.5430$) at the VD stage after overexpression of *nkx2.5* (Fig. 6E′). These results indicated that the reduction of ventricle size in *foxc1a*-null embryos may be due to the decrease of *nkx2.5* expression at cardiac progenitor specification stage, whereas there may be another mechanism that causes the increase of atrium size.

When the heat-shocked embryos grew to 108 hpf, they were measured to calculate their EI and SF. The results showed that the EI was significantly reduced ($p = 0.0012$) in *foxc1a*-null embryos, although it was significantly ($p < 0.0001$) increased in their wild-type siblings overexpressed with *nkx2.5* (Fig. 6F). In terms of SF, overexpression of *nkx2.5* by heat-shock activation significantly ($p = 0.005$) rescued the SF of *foxc1a*-null embryos but did not change ($p = 0.1030$) the SF of their wild-type siblings (Fig. 6G). Taken together, the results demonstrated that developmental stage–specific overexpression of *nkx2.5* partially rescued the ventricle morphogenesis and ventricular contraction defects caused by Foxc1a depletion.

Discussion

FOXC1, a bidirectional regulated transcription factor, plays important roles in many biological processes, such as eye development, circulatory system development, somitogenesis, and skeleton development, and its abnormal expression is involved in the progression of multiple cancers (4, 35–37). Previously, we reported that zebrafish *foxc1a*-knockout mutants displayed defective heart development (7). By analyzing the morphologic defects in details, we found that the *foxc1a*-null embryos exhibited disrupted heart structures and heart functions occurring from 50 hpf (Fig. 1) in addition to shorter body length and smaller eyes at 72 hpf (Fig. S1). The morphological defects were somehow similar to the phenotype of the heart, skeleton, and eye malformation in *Foxc1* knockout mice and patients carrying mutated *FOXC1* mutations (9). The results support the fact that zebrafish *foxc1a* is an ortholog of mammalian *Foxc1*, and they share conserved functions during vertebrate evolution.

It has been reported that zebrafish *foxc1a* has a duplicated copy named *foxc1b*. Double knockdown of *foxc1a* and *foxc1b* in zebrafish embryos results in loss of most vascular structure due to the reduced expression of the hemangioblast master regulator *etv2* and *tal1* in the rostral portion of ALPM of the morphants (38, 39). In this study, we found that the expressions of these two master regulators were almost not affected in the rostral portion of ALPM (Fig. 3*B, H, H′, J,* and *J′*); nor was the expression of endothelial marker gene *fli1a* (Fig. 3, *B, L,* and *L′*). Consistently, the artery, vein, and intersegment vessels in the trunk were formed normally in *foxc1a*-null embryos (Fig. S2). However, the angiogenesis in head was disrupted in *foxc1a*-null embryos (Fig. S2). The results suggested that *foxc1a/b* played redundant roles in the formation of only some vascular structure. Therefore, the vascular mechanism underlying the heart disorder of *foxc1a* mutants could not be completely ruled out.

Although there is visible blood flow in *foxc1a*-null zebrafish embryos from 30 hpf, erythrogenesis was disrupted with decreased expression of hemoglobin marker gene *hbae1* (Fig. S3, *C–F*). Considering the reduced expression of *tal1* in medial LPM (Fig. 3, *B, J,* and *J′*) of *foxc1a*-null embryos, we hypothesize that Foxc1a may regulate erythrogenesis by affecting the expression of the upstream master transcription factor *tal1*.

Nkx2-5 is one of the master transcriptional factors controlling vertebrate heart development. In human embryonic stem cells, knockdown of *FOXC1* leads to the decreased expression of marker genes for cardiac mesoderm, such as *Mef2c, Isl1,* and *Nkx2-5* (33). Consistent with this observation, the expression of the CPC marker gene *nkx2.5* was significantly decreased in the *foxc1a*-null embryos at 14 hpf (Fig. 3A), when cardiac progenitors are specified. By examining the expressions of *gata4/5/6* in the *foxc1a*-null embryos, we found the mutants had normal formation of ALPM (Fig. 3, *C–E* and *C′–E′*). Additionally, the expressions of both *pax2a*, a marker gene for posterior lateral plate mesoderm, and *hand2*, a second key regulator for the specification of cardiac progenitors, were normal in *foxc1a* mutants (Fig. 3, *F, F′, I,* and *I′*). These results are consistent with the observation that the germ layers were normally formed in *foxc1a*-null embryos, which suggests that Foxc1a is not involved in mesoderm formation but directs the specification of cardiac progenitors. Together with the finding that overexpression of *nkx2.5* is able to partially rescue the defective function of *foxc1a*-null embryos, our results demonstrate that *foxc1a* depletion affects the specification of cardiomyoblast in the caudal end of ALPM of zebrafish embryos by reducing the expression of *nkx2.5*.

Previously, researches have revealed that zebrafish *nkx* genes are essential for maintenance of ventricular identity (19). In mice, Nkx2-5 play a restrictive role in atrial myocyte proliferation. Nkx2-5 deficiency in the atria causes massive enlargement of working and conduction myocardium, leading to hyperplastic atrial myocardium (17). Consistent with *nkx2.5* mutants that

have defects of chamber differentiation, a dilated atrium and narrowed ventricle (19), we found in this study that the *foxc1a*-null zebrafish embryos also displayed a smaller ventricle and more inflated atrium, although the defective phenotype was not as severe as in *nkx2.5* mutants (Fig. 2, *A–D*). The mitigatory phenotype could be due to the residue expression of *nkx2.5* in *foxc1a*-null embryos. However, the abnormal atrial enlargement was not rescued by *nkx2.5* overexpression (Fig. 6). Taken
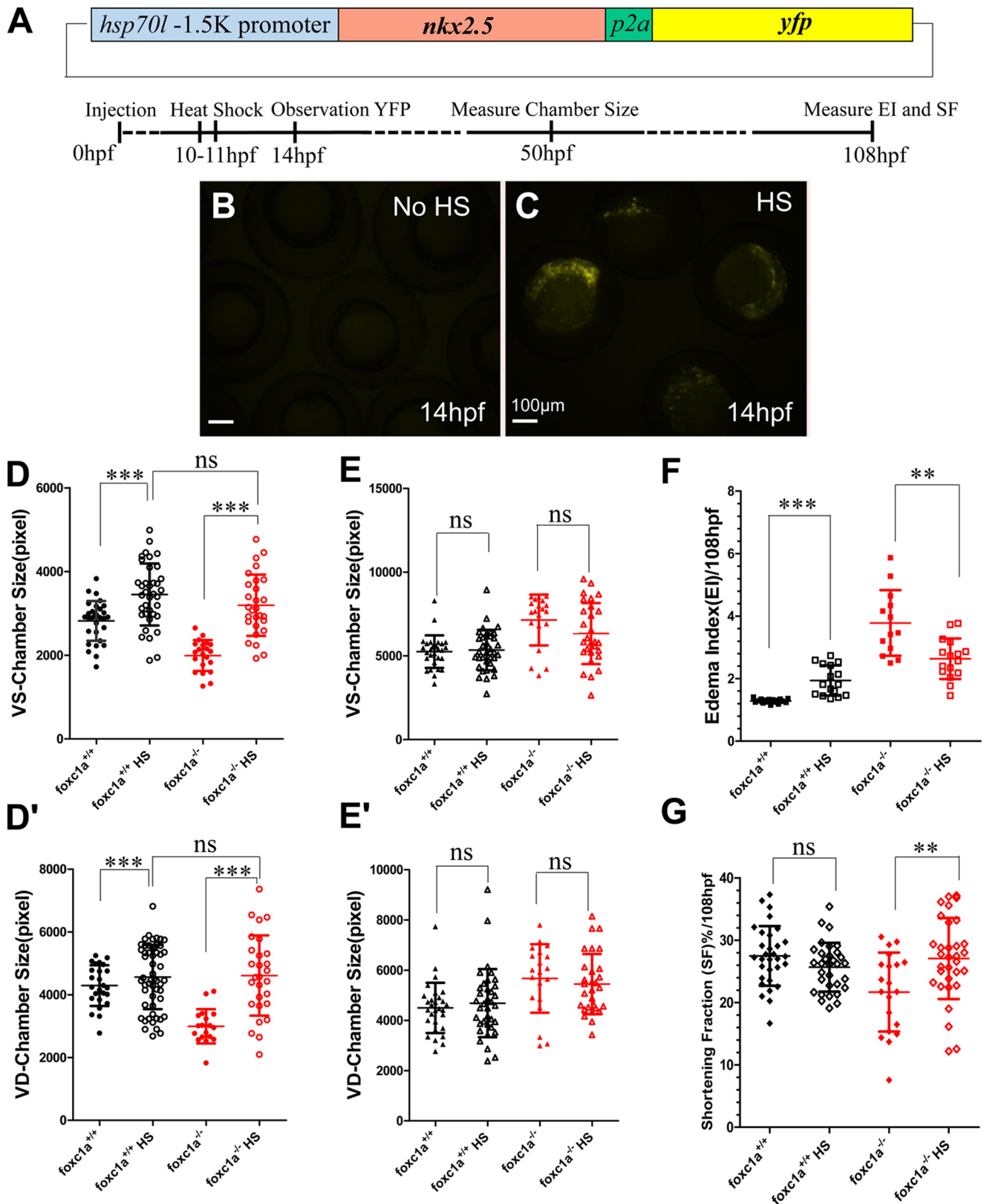
together, the results suggest that the atrial enlargement occurring in the *foxc1a*-null embryos might be caused by both the absence of *nkx2.5* expression and of cardiac dysfunction.

Although the expression of *nkx2.5* was significantly reduced in the caudal portion of ALPM in the *foxc1a*-null embryos, the expression area and mRNA level of *hand2*, a second marker gene of cardiac progenitor cells, was not changed in the ALPM (Fig. 3, *B, I,* and *I'*). The results suggest that Foxc1a deficiency would not affect the number of cardiac progenitor cells. Additionally, the previous research demonstrated that Nkx2.5 deficiency neither enhances the proliferation of atrial cells nor alters the patterns of cell death in embryos aged from 26 to 52 hpf (19). Therefore, similar to *nkx2.5* mutant zebrafish embryos, the cardiac chamber morphogenesis defects in *foxc1a* mutant zebrafish embryos probably result from the transdifferentiation of some ventricular cells into atrial cells. Considering that *foxc1a* is widely expressed in mesoderm and mesoderm-derived tissues (Fig. S5) and that the conventional knockout model of zebrafish *foxc1a* has its obvious limitation for investigating the molecular mechanism responsible for the heart defects, it will be very helpful to use a conditional knockout zebrafish to study the role of Foxc1a in zebrafish heart development in future studies.

Traditionally, FOX transcription factors regulate target genes by binding to the conserved core cis-element RYMAAYA in their promoter region (40). In zebrafish, Foxc1a is demonstrated to regulate the expression of *etv2* by binding to the canonical core sequence of (T/G)(G/C)(T/R)(T/Y)T(A/G)TTT in its enhancer region (39). Although there is a classic binding site, TGTTTGTTT, in the −506 bp position upstream of the zebrafish *nkx2.5* transcription start site, our results from the Dual-Luciferase activity assay revealed that deletion of this classic binding site did not affect the activation of Foxc1a on *nkx2.5* promoter (Fig. S6*B*). Performing a truncated promoter activity assay and ChIP assay in wild-type zebrafish embryos, we demonstrated that there were two non-canonical binding sites present in the zebrafish *nkx2.5* promoter (Fig. 5). Together with the results from double fluorescence *in situ* hybridization revealing that the expressions of *foxc1a* and *nkx2.5* were co-localized in some cells at ALPM of the embryos at both 12 and 14 hpf, we concluded that Foxc1a regulates the expression of *nkx2.5* directly.

It has been reported that *Foxc1-* and *Foxc2*-deficient mice exhibit a defective out-flow tract due to reduced *Tbx1* expression (40). Human patients carrying FOXC1 mutations suffer from cardiac anomalies, such as mild dysplasia of left ventricle, OFT, valvula tricuspidalis, and heart failure (10, 14, 18). These events suggest an important role of FOXC1 in second heart field development. The existence of the second heart field in zebrafish also has been verified (41, 42), and we also observed a shortened out-flow tract and dysplasia ventricle in the *foxc1a* mutant zebrafish embryos. These results indicate the conserved function of FOXC1 in the regulation of the second heart field among different species. However, we did not detect a change in *tbx1* expression at 14 hpf by transcriptome sequencing in *foxc1a* mutants (data not shown). This means that there may be another factor mediating the function of Foxc1a in zebrafish second heart field development. It has been reported that zebrafish second heart field development relies on the normal *nkx2.5* function (43), so we speculate that, compared to the mammalian Foxc1, zebrafish Foxc1a functions in second heart field development by directly regulating *nkx2.5* expression. Even so, more experiments should be performed to investigate whether the regulation of *nkx2.5* by Foxc1 is conserved in mammals.

Experimental procedures

Ethics statement

The experimental protocols involved in using zebrafish were approved by the institutional animal care and use committee at the Model Animal Research Center, Nanjing University. All animal experiments were performed in accordance with the National Institutes of Health Guidelines for the Care and Use of Laboratory Animals. Tubingen strain, transgenic zebrafish lines including $Tg(kdrl:eGFP)^{s843}$, $Tg(myl7:eGFP)^{m225}$, and $foxc1a^{nju19/+}$ mutant lines were used in this study.

Live imaging and quantification

To observe the morphology and count heart rates, we treated embryos with 0.04 mg/ml MS-222 (Sigma) at room temperature for 5 min and then mounted them with 3% methyl cellulose (Sigma). To examine the EI, we measured the distance from the heart center to the heart boundary (*a*) and from the heart center to the pericardium (*b*), as reported previously (28). The EI was calculated by the expression, *b/a*. The ventricular SF and heart chamber area were quantified and calculated in accordance with the reported method (44). Embryonic pictures were taken at VD and VS phases, respectively. The SF was computed by the equation, SF = (width of ventricle at VD − width of ventricle at VS)/width of ventricle × 100.

Heart rates of embryos were counted under a dissecting microscope (Leica). The frequency of heartbeat in each embryo was counted for 20 s, and the heart rate (beats/min) was calculated by multiplying by 3. By opening the files of the embryo

Figure 6. Heart defects in *foxc1a*-null embryos are partially rescued by overexpression of *nkx2.5* from 10 hpf. *A, schematic* of expression plasmid containing *Tg(−1.5hsp70l:nkx2.5-P2A-YFP)* and the workflow of the rescue experiment. *B,* no fluorescence was observed in the 14-hpf embryos microinjected with the expression plasmid containing *Tg(−1.5hsp70l:nkx2.5-P2A-YFP)* into the embryos at the one-cell stage. *C,* eYFP expression was observed in the 14-hpf embryos microinjected with the expression plasmid at the one-cell stage and heat-shocked from 10 to 11 hpf. *D, E, D',* and *E',* scatter plot showing the ventricle (*dot*) size was observed at VS (*D*) and VD (*D'*) phases, and the atrium (*triangle*) size was observed at VS (*E*) and VD (*E'*) phases, respectively. The *solid dot* and *triangle* (*D, D', E,* and *E'*) indicate the embryos without heat shock. The *open dot* and *triangle* (*D, D', E,* and *E'*) indicate the embryos with heat shock (*n* = 24 in wild-type embryos (*black*) and *n* = 18 in mutants (*red*)). *F,* scatter plot showing the EI of no-heat-shock control embryos and heat-shock ones at 108 hpf. The *black solid boxes* indicate wild-type siblings without heat shock (*n* = 15); the *black open boxes* indicate wild-type siblings with heat shock (*n* = 16); the *red solid boxes* denote *foxc1a* mutants without heat shock (*n* = 13); the *red open boxes* denote *foxc1a* mutants with heat shock (*n* = 16). *G,* scatter plot showing the ventricle shortening fraction of no-heat-shock control embryos and heat-shock ones at 108 hpf. The *black solid rhombi* indicate wild type sibling without heat shock (*n* = 32); *black open rhombi* indicate wild-type sibling with heat shock (*n* = 31); *red solid rhombi* denote *foxc1a* mutants without heat shock (*n* = 20); *black open rhombi* denote *foxc1a* mutants with heat shock (*n* = 32). *HS,* heat shock. **, $p < 0.01$; ***, $p < 0.001$; *ns,* not significant. *Error bars,* S.D.

ASBMB

J. Biol. Chem. (2018) 293(2) 638–650 **647**

photos taken at different phases with Photoshop software, we measured the chamber area by marking the ventricle and atrium region.

Histological section and staining

Zebrafish embryos were fixed with 4% paraformaldehyde at 4 °C for >24 h. The fixed embryos were dehydrated with gradient ethanol, cleared with xylene, and then embedded in paraffin. Embedded embryos were cut as series of sections with 5-μm thickness, as in our previous report (30). The sections were placed on glass slides and stained with hematoxylin and eosin. Photomicrographs were taken using a DP70 digital camera under a dissecting microscope (Olympus). At least three consecutive sections were observed to ascertain that the sections contained the embryonic heart structures.

With regard to *o*-dianisidine staining, embryos were collected at 50 hpf and incubated with *o*-dianisidine solution for 15 min in the dark. *o*-Dianisidine solution contained 0.6 mg/ml *o*-dianisidine, 0.01 M sodium acetate (pH 4.5), 0.65% H_2O_2, and 40% ethanol (v/v). Embryos were embedded with glycerol, and photographs were taken with a DP70 digital camera (Olympus).

Whole-transcriptome deep sequencing

Total RNA was isolated from single offspring of *foxc1a*$^{nju19/+}$ zebrafish incross using TRIzol reagent (Invitrogen). The cDNA synthesized from total RNA isolated from a single embryo by reverse transcriptase (Vazyme) was used as the template of PCR to genotype *foxc1a* alleles, as we reported previously (7). After genotyping, 5 μg of total RNA was collected from wild-type siblings and *foxc1a* mutants for RNA deep sequencing, respectively. The transcriptome sequencing was performed by Novel-Bio Bio-Pharm Technology Co. (Shanghai, China). Gene expression levels were quantified by RPKM (reads per kilobase of transcript per million mapped reads) arithmetic. MapSplice software was used for data alignment, and EB-Seq arithmetic was used for the screening of differential expression genes.

Whole-mount in situ hybridizations (ISHs) and double fluorescence ISHs

Whole-mount ISHs were performed as we described previously (7). The templates for making RNA probes to detect the expressions of *nkx2.5* (NM_131421.1), *hand2* (NM_131626.3), *pax2a* (NM_131184.2), *klf2a* (NM_131856.3), *hbae1* (NM_182940.2), *foxc1a* (NM_131728.3), *fli1a* (NM_131348.2), *ta* (NM_131162.1), *gsc* (NM_131017.1), *dkk1b* (NM_131003.1), *noto* (NM_131055.1), *mixl1* (NM_130940.3), *sox32* (NM_131851.1), *sox17* (NM_131287.2), and *zic1* (NM_130933.1) were cloned, respectively, from RT-PCR products. The primers used for RT-PCR are listed in Table S1. RNA probes for detecting the expressions of *amhc* (NM_198823.1), *vmhc* (NM_001112733.1), *myl7* (NM_131329.3), *nppa* (NM_198800.3), *bmp4* (NM_131342.2), *vcana* (NM_001326557.1), *notch1b* (NM_131302.2), *has2* (NM_153650.2), *gata4* (NM_131236.2), *gata5* (NM_131235.2), and *gata6* (NM_131557.2) were prepared as described previously (30, 45). After hybridization, each embryo was photographed under a dissecting microscope using a digital camera. The genotype of each hybridized embryo was then determined by PCR amplification as we reported previously (7).

The method of double fluorescence ISHs was used as in the previous report (46). Briefly, the wild-type embryos were fixed at 12 and 14 hpf with 4% paraformaldehyde overnight. After dehydration and protease K treatment, the embryos were then hybridized with *nkx2.5* and *ta* RNA probe labeled with digoxin and *foxc1a* RNA probe labeled with fluorescein at 65 °C overnight. After the removal of probe, the anti-fluorescein conjugated with peroxidase antibody (1:500; Roche Applied Science) along with TSA plus fluorescein solution (1:50; PerkinElmer Life Sciences) was added. Then the anti-digoxin conjugated with peroxidase antibody (1:1000; Roche Applied Science) along with TSA plus Cy5 solution (1:50; PerkinElmer Life Sciences) was added. After inactivation of the primary antibody, the embryos were then flatted and placed on the glass slides, and images were photographed with a TCS SP5 confocal microscope (Leica).

In vitro synthesis of foxc1a mRNA

To synthesize mRNA *in vitro*, we first cloned the full-length coding sequences of wild-type and mutant *foxc1a* (NM_131728.3) from wild-type zebrafish and *foxc1a* mutants by RT-PCR. The cDNAs were cloned into pGEM-T easy vector (Promega) using Phanta Super-Fidelity DNA Polymerase (Vazyme), and then their identities were confirmed by direct sequencing from both ends. The capped and tailed mRNA was synthesized from the linearized vector by NcoI (Thermo) using the mMES-SAGE mMACHINE Sp6 Ultra Kit (Ambion). The synthesized mRNAs were further purified with the MEGAclear™ Transcription Clean-Up Kit (Ambion) to remove the free nucleotides.

Quantitative real-time PCR

Quantitative real-time PCR was performed to examine the relative expression levels of *gata4* (NM_131236.2), *gata5* (NM_131235.2), *gata6* (NM_131557.2), *etv2* (NM_001037375.1), *tal1* (NM_213237.1), *nkx2.5* (NM_131421.1), *hand2* (NM_131626.3), *fli1a* (NM_131348.2), and *gata1* (NM_131234.1) using the ABI Prism 7300 sequence detector (PE Biosystems). The quantitative real-time PCR primers used in the assay are listed in Table S2 or in the previous report (46). Total RNAs were extracted from a single embryo using TRIzol reagent (Invitrogen) for each assay. RNA was reverse-transcribed (Vazyme) into cDNA. The cDNA was then used as template to genotype *foxc1a* alleles and to perform real-time PCR using the SYBR Green method following the manufacturer's protocol (Roche Applied Science). The relative expression levels of *gata4/5/6* were normalized by the expression of *actb1* (NM_131031.1), and those of *etv2*, *tal1*, *nkx2.5*, *hand2*, *fli1a*, and *gata1* were normalized by the expression of *hprt1* (NM_212986.1).

Promoter construction and Dual-Luciferase assay

Zebrafish *nkx2.5* promoters with different lengths were individually cloned into pGL3 basic vector linearized with NcoI and XhoI (Thermo). To test the promoter activity in response to Foxc1a, we microinjected 50 pg of luciferase vectors, 1 pg of *Renilla* expression vectors, and 20 pg of wild-type *foxc1a* mRNA or 20 pg of *foxc1a* mutant mRNA into wild-type

embryos at the one-cell stage. Embryos were then collected at 10 hpf and lysed with passive lysis buffer (Promega).

ChIP-PCR

To perform the ChIP assay, we collected the wild-type zebrafish embryos at the 8–10-somite stage. 5 µg of FOXC1 antibody (GTX25079, GeneTex) was used to immunoprecipitate all genomic DNA crossed with Foxc1a protein, and 1 µg of mouse IgG was used as control. The ChIP-PCR assay was performed using the EZ-ChIP chromatin immunoprecipitation kit (Millipore) following the manufacturer's instructions. The semiquantitative PCR was performed as follows. The PCR conditions were 95 °C for 5 min; 35 cycles of 95 °C for 30 s, 52 °C for 30 s, 72 °C for 15 s; and 72 °C 10 min. The PCR products were then subjected to separation by 2% agarose electrophoresis. The primers for PCR are listed in Table S3.

Statistics

Data are presented as mean ± S.D. Statistical significance was determined using the unpaired two-tailed t test. A value of $p < 0.05$ (*) was considered statistically significant, and $p < 0.01$ (**) and $p < 0.001$ (***) were considered statistically very significant.

References

1. Keegan, B. R., Meyer, D., and Yelon, D. (2004) Organization of cardiac chamber progenitors in the zebrafish blastula. *Development* **131,** 3081–3091 CrossRef Medline
2. Berry, F. B., Saleem, R. A., and Walter, M. A. (2002) Foxc1 transcriptional regulation is mediated by N- and C-terminal activation domains and contains a phosphorylated transcriptional inhibitory domain. *J. Biol. Chem.* **277,** 10292–10297 CrossRef Medline
3. Kume, T., Deng, K. Y., Winfrey, V., Gould, D. B., Walter, M. A., and Hogan, B. L. (1998) The forkhead/winged helix gene mf1 is disrupted in the pleiotropic mouse mutation congenital hydrocephalus. *Cell* **93,** 985–996 CrossRef Medline
4. Kume, T., Jiang, H., Topczewska, J. M., and Hogan, B. L. (2001) The murine winged helix transcription factors, foxc1 and foxc2, are both required for cardiovascular development and somitogenesis. *Genes Dev.* **15,** 2470–2482 CrossRef Medline
5. Seo, S., and Kume, T. (2006) Forkhead transcription factors, foxc1 and foxc2, are required for the morphogenesis of the cardiac outflow tract. *Dev. Biol.* **296,** 421–436 CrossRef Medline
6. Kume, T. (2009) The cooperative roles of foxc1 and foxc2 in cardiovascular development. *Adv. Exp. Med. Biol.* **665,** 63–77 CrossRef Medline
7. Li, J., Yue, Y., Dong, X., Jia, W., Li, K., Liang, D., Dong, Z., Wang, X., Nan, X., Zhang, Q., and Zhao, Q. (2015) Zebrafish foxc1a plays a crucial role in early somitogenesis by restricting the expression of aldh1a2 directly. *J. Biol. Chem.* **290,** 10216–10228 CrossRef Medline
8. Honkanen, R. A., Nishimura, D. Y., Swiderski, R. E., Bennett, S. R., Hong, S., Kwon, Y. H., Stone, E. M., Sheffield, V. C., and Alward, W. L. (2003) A family with axenfeld-rieger syndrome and peters anomaly caused by a point mutation (phe112ser) in the foxc1 gene. *Am. J. Ophthalmol.* **135,** 368–375 CrossRef Medline
9. Gripp, K. W., Hopkins, E., Jenny, K., Thacker, D., and Salvin, J. (2013) Cardiac anomalies in axenfeld-rieger syndrome due to a novel foxc1 mutation. *Am. J. Med. Genet. A* **161A,** 114–119 CrossRef Medline
10. Du, R. F., Huang, H., Fan, L. L., Li, X. P., Xia, K., and Xiang, R. (2015) A novel mutation of foxc1 (r127l) in an axenfeld-rieger syndrome family with glaucoma and multiple congenital heart diseases. *Ophthalmic Genet.* **37,** 111–115 CrossRef
11. Lambers, E., and Kume, T. (2016) Navigating the labyrinth of cardiac regeneration. *Dev. Dyn.* **245,** 751–761 CrossRef Medline
12. Hannenhalli, S., Putt, M. E., Gilmore, J. M., Wang, J., Parmacek, M. S., Epstein, J. A., Morrisey, E. E., Margulies, K. B., and Cappola, T. P. (2006) Transcriptional genomics associates fox transcription factors with human heart failure. *Circulation* **114,** 1269–1276 CrossRef Medline
13. Yeo, H. C., Ting, S., Brena, R. M., Koh, G., Chen, A., Toh, S. Q., Lim, Y. M., Oh, S. K., and Lee, D. Y. (2016) Genome-wide transcriptome and binding sites analyses identify early fox expressions for enhancing cardiomyogenesis efficiency of hesc cultures. *Sci. Rep.* **6,** 31068 CrossRef Medline
14. Zhu, H. (2016) Forkhead box transcription factors in embryonic heart development and congenital heart disease. *Life Sci.* **144,** 194–201 CrossRef Medline
15. Biben, C., Weber, R., Kesteven, S., Stanley, E., McDonald, L., Elliott, D. A., Barnett, L., Köentgen, F., Robb, L., Feneley, M., and Harvey, R. P. (2000) Cardiac septal and valvular dysmorphogenesis in mice heterozygous for mutations in the homeobox gene nkx2-5. *Circ. Res.* **87,** 888–895 CrossRef Medline
16. Jay, P. Y., Berul, C. I., Tanaka, M., Ishii, M., Kurachi, Y., and Izumo, S. (2003) Cardiac conduction and arrhythmia: Insights from nkx2.5 mutations in mouse and humans. *Novartis Found. Symp.* **250,** 227–238; discussion 238–241, 276–279 CrossRef Medline
17. Nakashima, Y., Yanez, D. A., Touma, M., Nakano, H., Jaroszewicz, A., Jordan, M. C., Pellegrini, M., Roos, K. P., and Nakano, A. (2014) Nkx2-5 suppresses the proliferation of atrial myocytes and conduction system. *Circ. Res.* **114,** 1103–1113 CrossRef Medline
18. George, V., Colombo, S., and Targoff, K. L. (2015) An early requirement for nkx2.5 ensures the first and second heart field ventricular identity and cardiac function into adulthood. *Dev. Biol.* **400,** 10–22 CrossRef Medline
19. Targoff, K. L., Colombo, S., George, V., Schell, T., Kim, S. H., Solnica-Krezel, L., and Yelon, D. (2013) Nkx genes are essential for maintenance of ventricular identity. *Development* **140,** 4203–4213 CrossRef Medline
20. Schott, J. J., Benson, D. W., Basson, C. T., Pease, W., Silberbach, G. M., Moak, J. P., Maron, B. J., Seidman, C. E., and Seidman, J. G. (1998) Congenital heart disease caused by mutations in the transcription factor nkx2-5. *Science* **281,** 108–111 CrossRef Medline
21. Goldmuntz, E., Geiger, E., and Benson, D. W. (2001) Nkx2.5 mutations in patients with tetralogy of Fallot. *Circulation* **104,** 2565–2568 CrossRef Medline
22. Tong, Y. F. (2016) Mutations of nkx2.5 and gata4 genes in the development of congenital heart disease. *Gene* **588,** 86–94 CrossRef Medline
23. Keegan, B. R., Feldman, J. L., Begemann, G., Ingham, P. W., and Yelon, D. (2005) Retinoic acid signaling restricts the cardiac progenitor pool. *Science* **307,** 247–249 CrossRef Medline
24. Lin, S. C., Dollé, P., Ryckebüsch, L., Noseda, M., Zaffran, S., Schneider, M. D., and Niederreither, K. (2010) Endogenous retinoic acid regulates cardiac progenitor differentiation. *Proc. Natl. Acad. Sci. U.S.A.* **107,** 9234–9239 CrossRef Medline
25. Jain, R., Li, D., Gupta, M., Manderfield, L. J., Ifkovits, J. L., Wang, Q., Liu, F., Liu, Y., Poleshko, A., Padmanabhan, A., Raum, J. C., Li, L., Morrisey, E. E., Lu, M. M., Won, K. J., and Epstein, J. A. (2015) Heart development: integration of bmp and wnt signaling by hopx specifies commitment of cardiomyoblasts. *Science* **348,** aaa6071 CrossRef Medline
26. Chang, S. W., Mislankar, M., Misra, C., Huang, N., Dajusta, D. G., Harrison, S. M., McBride, K. L., Baker, L. A., and Garg, V. (2013) Genetic abnormalities in foxp1 are associated with congenital heart defects. *Hum Mutat.* **34,** 1226–1230 CrossRef Medline
27. Nie, J., Jiang, M., Zhang, X., Tang, H., Jin, H., Huang, X., Yuan, B., Zhang, C., Lai, J. C., Nagamine, Y., Pan, D., Wang, W., and Yang, Z. (2015) Post-

SASBMB

J. Biol. Chem. (2018) 293(2) 638–650 **649**

transcriptional regulation of nkx2-5 by rhau in heart development. *Cell Rep.* **13,** 723–732 CrossRef Medline

28. Li, J., Jia, W., and Zhao, Q. (2014) Excessive nitrite affects zebrafish valvulogenesis through yielding too much no signaling. *PLoS One* **9,** e92728 CrossRef Medline

29. Vermot, J., Forouhar, A. S., Liebling, M., Wu, D., Plummer, D., Gharib, M., and Fraser, S. E. (2009) Reversing blood flows act through klf2a to ensure normal valvulogenesis in the developing heart. *PLoS Biol.* **7,** e1000246 CrossRef Medline

30. Li, J., Yue, Y., and Zhao, Q. (2016) Retinoic acid signaling is essential for valvulogenesis by affecting endocardial cushions formation in zebrafish embryos. *Zebrafish* **13,** 9–18 CrossRef Medline

31. Combs, M. D., and Yutzey, K. E. (2009) Heart valve development: regulatory networks in development and disease. *Circ. Res.* **105,** 408–421 CrossRef Medline

32. Staudt, D., and Stainier, D. (2012) Uncovering the molecular and cellular mechanisms of heart development using the zebrafish. *Annu. Rev. Genet.* **46,** 397–418 CrossRef Medline

33. Lambers, E., Arnone, B., Fatima, A., Qin, G., Wasserstrom, J. A., and Kume, T. (2016) Foxc1 regulates early cardiomyogenesis and functional properties of embryonic stem cell derived cardiomyocytes. *Stem Cells* **34,** 1487–1500 CrossRef Medline

34. Li, J., Zhang, B. B., Ren, Y. G., Gu, S. Y., Xiang, Y. H., and Du, J. L. (2015) Intron targeting-mediated and endogenous gene integrity-maintaining knockin in zebrafish using the crispr/cas9 system. *Cell Res.* **25,** 634–637 CrossRef Medline

35. Berry, F. B., Lines, M. A., Oas, J. M., Footz, T., Underhill, D. A., Gage, P. J., and Walter, M. A. (2006) Functional interactions between foxc1 and pitx2 underlie the sensitivity to foxc1 gene dose in axenfeld-rieger syndrome and anterior segment dysgenesis. *Hum. Mol. Genet.* **15,** 905–919 CrossRef Medline

36. Du, J., Li, L., Ou, Z., Kong, C., Zhang, Y., Dong, Z., Zhu, S., Jiang, H., Shao, Z., Huang, B., and Lu, J. (2012) Foxc1, a target of polycomb, inhibits metastasis of breast cancer cells. *Breast Cancer Res. Treat.* **131,** 65–73 CrossRef Medline

37. Han, B., Qu, Y., Jin, Y., Yu, Y., Deng, N., Wawrowsky, K., Zhang, X., Li, N., Bose, S., Wang, Q., Sakkiah, S., Abrol, R., Jensen, T. W., Berman, B. P., Tanaka, H., *et al.* (2015) Foxc1 activates smoothened-independent hedgehog signaling in basal-like breast cancer. *Cell Rep.* **13,** 1046–1058 CrossRef Medline

38. De Val, S., Chi, N. C., Meadows, S. M., Minovitsky, S., Anderson, J. P., Harris, I. S., Ehlers, M. L., Agarwal, P., Visel, A., Xu, S. M., Pennacchio, L. A., Dubchak, I., Krieg, P. A., Stainier, D. Y., and Black, B. L. (2008) Combinatorial regulation of endothelial gene expression by ets and forkhead transcription factors. *Cell* **135,** 1053–1064 CrossRef Medline

39. Veldman, M. B., and Lin, S. (2012) Etsrp/etv2 is directly regulated by foxc1a/b in the zebrafish angioblast. *Circ. Res.* **110,** 220–229 CrossRef Medline

40. Kaufmann, E., Müller, D., and Knöchel, W. (1995) DNA recognition site analysis of *Xenopus* winged helix proteins. *J. Mol. Biol.* **248,** 239–254 CrossRef Medline

41. Lazic, S., and Scott, I. C. (2011) Mef2cb regulates late myocardial cell addition from a second heart field-like population of progenitors in zebrafish. *Dev. Biol.* **354,** 123–133 CrossRef Medline

42. Zhou, Y., Cashman, T. J., Nevis, K. R., Obregon, P., Carney, S. A., Liu, Y., Gu, A., Mosimann, C., Sondalle, S., Peterson, R. E., Heideman, W., Burns, C. E., and Burns, C. G. (2011) Latent TGF-β binding protein 3 identifies a second heart field in zebrafish. *Nature* **474,** 645–648 CrossRef Medline

43. Guner-Ataman, B., Paffett-Lugassy, N., Adams, M. S., Nevis, K. R., Jahangiri, L., Obregon, P., Kikuchi, K., Poss, K. D., Burns, C. E., and Burns, C. G. (2013) Zebrafish second heart field development relies on progenitor specification in anterior lateral plate mesoderm and nkx2.5 function. *Development* **140,** 1353–1363 CrossRef Medline

44. Hoage, T., Ding, Y., and Xu, X. (2012) Quantifying cardiac functions in embryonic and adult zebrafish. *Methods Mol. Biol.* **843,** 11–20 CrossRef Medline

45. Liang, D., Jia, W., Li, J., Li, K., and Zhao, Q. (2012) Retinoic acid signaling plays a restrictive role in zebrafish primitive myelopoiesis. *PLoS One* **7,** e30865 CrossRef Medline

46. Brend, T., and Holley, S. A. (2009) Zebrafish whole mount high-resolution double fluorescent *in situ* hybridization. *J. Vis. Exp.* CrossRef Medline

ASBMB